
Phase I, First-in-Human Study of BMS747158, a Novel ^{18}F -Labeled Tracer for Myocardial Perfusion PET: Dosimetry, Biodistribution, Safety, and Imaging Characteristics After a Single Injection at Rest

Jamshid Maddahi^{1,2}, Johannes Czernin¹, Joel Lazewatsky³, Sung-Cheng Huang¹, Magnus Dahlbom¹, Heinrich Schelbert¹, Richard Sparks⁴, Alexander Ehlgren³, Paul Crane³, Qi Zhu³, Marybeth Devine³, and Michael Phelps¹

¹Department of Molecular and Medical Pharmacology (Nuclear Medicine), David Geffen School of Medicine at University of California, Los Angeles, California; ²Department of Medicine (Cardiology), David Geffen School of Medicine at University of California, Los Angeles, California; ³Lantheus Medical Imaging, Billerica, Massachusetts; and ⁴CDE Dosimetry Services, Knoxville, Tennessee

^{18}F -labeled BMS747158 is a novel myocardial perfusion imaging tracer that targets mitochondrial complex 1. The objectives of this phase I study were to evaluate radiation dosimetry, biodistribution, human safety, tolerability, and early elimination of ^{18}F activity in urine after injection of a single dose of the tracer at rest in healthy subjects. **Methods:** Thirteen healthy subjects were injected with 170–244 MBq (4.6–6.6 mCi) of BMS747158 intravenously. Dynamic PET was obtained over the heart for 10 min, followed by sequential whole-body imaging for 5 h. Blood samples and urinary excretion were collected for up to 8 h. Heart rate, electrocardiogram, and blood pressure were monitored before and during imaging. The residence times were determined from multiexponential regression of organ region-of-interest data normalized by injected dose. Absorbed dose estimates for all target organs were determined using MIRD schema with OLINDA/EXM software. **Results:** The organ receiving the largest mean absorbed dose was the kidneys at 0.066 mSv/MBq (0.24 rem/mCi), followed by the heart wall at 0.048 mSv/MBq (0.18 rem/mCi). The mean effective dose was 0.019 mSv/MBq (0.072 rem/mCi). The heart exhibited high and sustained retention of BMS747158 from the earliest images through approximately 5 h after injection. There were no drug-related adverse events, and the tracer was well tolerated in all subjects. Mean urinary excretion was 4.83 percentage injected dose (range, 0.64–12.41 percentage injected dose). **Conclusion:** These preliminary data suggest that ^{18}F -labeled BMS747158 appears to be well tolerated and has a unique potential for myocardial perfusion PET.

Key Words: ^{18}F -labeled BMS747158; myocardial perfusion imaging; mitochondrial complex 1

J Nucl Med 2011; 52:1490–1498
DOI: 10.2967/jnumed.111.092528

Received Apr. 29, 2011; revision accepted May 3, 2011.
For correspondence or reprints contact: Jamshid Maddahi, 100 UCLA Medical Plaza, Ste. 410, Los Angeles, CA 90095-7064.
E-mail: jmaddahi@mednet.ucla.edu
Published online Aug. 17, 2011.
Guest Editor: Richard Brunken, Cleveland Clinic Foundation
COPYRIGHT © 2011 by the Society of Nuclear Medicine, Inc.

Coronary artery disease is a major cause of death in modern industrialized countries. Assessments of regional myocardial perfusion at rest and during stress (exercise or pharmacologic coronary vasodilation) have proved valuable for noninvasive diagnosis of coronary artery disease. Myocardial perfusion imaging (MPI) with PET has been shown to be superior to SPECT (1–3). Nevertheless, widespread clinical use of PET MPI has been limited by the currently available PET myocardial perfusion tracers.

Several PET blood flow tracers, such as ^{82}Rb -chloride, ^{13}N -ammonia, and ^{15}O -water, have been developed and validated for assessment of myocardial perfusion (4–6). ^{13}N and ^{15}O are cyclotron-produced tracers with short half-lives of 10 and 2 min, respectively. Therefore, their use is limited to facilities with an onsite cyclotron. Although ^{82}Rb is a generator-produced tracer, its short half-life of 1.2 min, the high cost of the generator, and the inability to perform studies in conjunction with treadmill exercise have limited its widespread use.

These limitations of the current myocardial perfusion PET tracers have created a need for a new perfusion agent with improved properties (7). An optimal myocardial perfusion PET tracer that is retained by tissue in proportion to capillary perfusion should have a high first-pass extraction fraction from blood to tissue and retention in cardiac tissue, with a low clearance rate from tissue to blood (unidirectional extraction and retention) over a wide range of myocardial blood flow (MBF); rapid clearance from blood to minimize spillover in the image from the blood pool to myocardial tissue; and minimal uptake and retention in the lungs and liver to minimize spillover from these tissues to myocardial tissue.

The better tracers are at meeting these criteria, the more accurate are the estimates of absolute MBF, and the higher the contrast between myocardial tissue and surrounding tissues to permit detection of mild decreases in coronary flow

and flow reserve. The tracer should also have characteristics that allow supply as a unit dose from regional PET radio-pharmacies that supply ^{18}F -labeled FDG, obviating onsite cyclotrons or costly ^{82}Rb generators. Furthermore, it should also allow imaging during exercise.

BMS747158 is a novel ^{18}F -labeled PET MBF tracer. This agent is a structural analog of pyridaben and binds to mitochondrial complex 1 with high affinity (Fig. 1) (8). Because mitochondria constitute 20%–30% of the myocardial intracellular volume, molecules that target mitochondrial proteins will have high target density and be selectively retained in the myocardium. In preclinical studies, BMS747158 has been shown to have a higher first-pass extraction fraction than ^{201}Tl - and $^{99\text{m}}\text{Tc}$ -sestamibi at high flow rates (9). Thus, BMS747158 has the potential to yield steady-state myocardial imaging with the improved resolution and quantification afforded by PET. BMS747158 also could provide improved clinical utility and ease of use because of the longer half-life (110 min) of an ^{18}F -based tracer that makes delivery of unit doses from regional PET pharmacies feasible. Preclinical studies using BMS747158 PET MPI showed superior extraction and prolonged retention versus MBF, compared with nuclear tracers used in SPECT MPI (8–11).

The primary objective of this study was to estimate the radiation dosimetry of a single dose of BMS747158 tracer in healthy subjects. The secondary objective was to assess biodistribution, safety, tolerability, and early elimination of ^{18}F activity in urine after a single injection of BMS747158.

MATERIALS AND METHODS

Study Population

Healthy adults (as determined by medical history, physical examination, vital signs, electrocardiogram [ECG], electroencephalogram [EEG], neurologic examination, and clinical laboratory testing), aged 18–40 y, participated in the study. Subjects had to meet all protocol-specified inclusion criteria and none of the exclusion criteria. Subjects were to be men or women, aged 18–40 y inclusive, with a body mass index of 18–30 kg/m^2 , with no clinically significant deviation from reference ranges in physical examination, ECG, EEG, and clinical laboratory parameters. All subjects who were women of child-bearing potential were nonpregnant and were using an adequate and medically approved method of contraception to avoid pregnancy for at least 1 mo before study enrollment through 1 mo after dosing and had a negative serum pregnancy test within 24 h before dose administration.

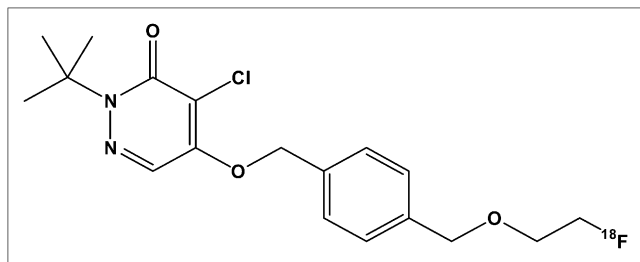


FIGURE 1. Structure of BMS747158.

Subjects were excluded if they had any significant active or chronic medical illness or recent significant trauma or any condition that may have disrupted or increased permeability of the blood–brain barrier; any major surgery within 4 wk before enrollment or planned within 2 wk after completion of the study; a donation of blood or plasma to a blood bank or for a clinical study within 4 wk before enrollment; a blood transfusion within 4 wk of enrollment; any oral, transdermal, implanted, or injectable contraceptive hormones or hormone replacement therapy within 3 mo; and any radiopharmaceutical within a period equal to 10 half-lives of the isotope. Subjects were excluded if they had a positive urine screen for drugs of abuse at screening or before dosing or used any drugs (including over-the-counter medications and herbal preparations) within 2 wk before enrollment; if they had anticipated using drugs during the enrollment period through study follow-up; or for any for other sound medical, psychiatric, or social reason as determined by the principal investigator.

Study Design

This was a phase I, nonrandomized, open-label, single-dose study. Thirteen healthy adult subjects were enrolled and administered a single dose of BMS747158 at a single study center in the United States (UCLA Medical Center). Subjects were screened within 14 d before enrollment to confirm eligibility and began baseline assessments at the study center the day before study drug administration. Subjects remained at the study center until completion of the study day 2 safety assessments (24 ± 8 h after dosing). A telephone call was made to study subjects 48 ± 8 h after dosing for monitoring of adverse events (AEs). All subjects returned to the study center approximately 1 wk (5–7 d) after dosing for a follow-up safety visit and were contacted by telephone approximately 14–17 d after dosing for final monitoring of serious AEs. The major study events are displayed in Figure 2.

Determination of Dose and Method of Administration

The intravenous bolus injection was calculated to deliver no more than 8 mCi of ^{18}F at the time of injection. The mean (\pm SD) final decay-corrected dose was 222 ± 22.2 MBq (6 ± 0.6 mCi) of ^{18}F , with a range of 170–244 MBq (4.6–6.6 mCi). The difference between the target dose and the final dose was due to the retention of BMS747158 in the syringe. The 296-MBq (8-mCi) target dose was selected to provide adequate count statistics and was projected to be well below the maximum acceptable radiation exposure based on preclinical data. These data demonstrated that the maximum dose of BMS747158 that may be administered to a human without exceeding 50 mSv (5 rem) to the target was 742 MBq (20.0 mCi), and the injected dose that yielded an effective dose (ED) of 10 mSv (1 rem) or less was 666 MBq (18.0 mCi) (12).

On day 1, each subject received a 1- to 3-mL intravenous bolus injection of ^{18}F -BMS747158 in a sterile solution of 5% or less ethanol containing 50 mg or less of sodium ascorbate per milliliter in water, calculated to deliver approximately the target dose of BMS747158 at the time of injection. The dose was administered in less than 10 s, followed immediately by a 3- to 5-mL saline flush. The net injected dose was calculated by subtracting the decay-corrected radioactivity in the syringe and injection tubing after injection from the assayed and decay-corrected radioactivity in the syringe before injection. The mass of BMS747158 tracer administered was 0.57 ± 0.1 μg .

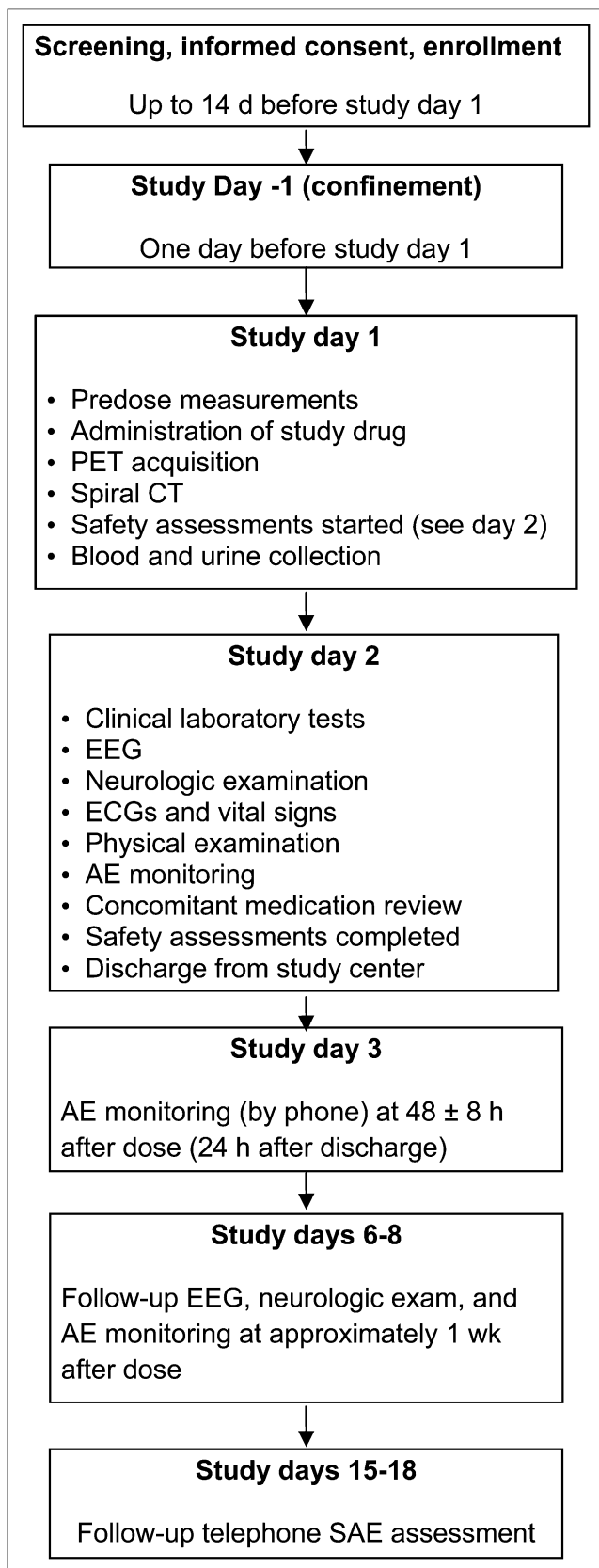


FIGURE 2. Study events overview. SAE = serious adverse event.

PET Protocol

Whole-body PET from head to mid thigh was performed in 2-dimensional format at protocol-specified time windows outlined in Table 1 using a Siemens ECAT HR+ system and applying corrections for attenuation, randoms, and scatter. A low- to moderate-resolution spiral CT scan, from upper chest to lower abdomen, was obtained before or after the PET session to aid in organ identification and volume assessment, if needed.

Dosimetry Analyses

Estimates of radiation dosimetry for the standard organs of the adult male and female models and for the salivary glands, as well as the effective dose equivalent (13) and ED (14), were determined using the OLINDA/EXM software (15). Assessment of radiation dosimetry was based on the MIRD method, with data derived from imaging studies, using methods consistent with MIRD pamphlet no. 16 (16).

The attenuation-corrected transverse image data slice planes were combined into a single 3-dimensional image matrix for each subject and each time point using custom software. These images were then divided into 6 image sets (anterior, posterior, salivary, thyroid, source, and full) of combined coronal plane image data for each subject at each time point, grouping organs with similar anterior-to-posterior depths to optimize the region-of-interest (ROI) creation and minimize background contribution to the organs contained in each combined coronal plane image. The anterior images contained stomach wall, heart wall, and urinary bladder. The posterior images contained kidneys, lumbar spine, and spleen (when visible). The salivary images contained the salivary glands (parotid and submandibular). The thyroid images contained the thyroid. The full images combined all of the coronal image planes that contained subject image data and were used for quantification of the brain and liver. The source images contained the calibration source.

ROIs were drawn around all organs that showed uptake above background using custom software developed and validated for this purpose. Absolute radioactivity was determined by normalizing ROI sums by a calibration factor derived from the calibration source. Region counts were also adjusted for activity containing underlying and overlying tissue that was not part of the organ or tissue being quantified by use of background ROIs. Total body region counts were also corrected for off-body background counts. Appropriate normalization of region sizes for organ and adjacent regions were made. Unobstructed regions of organs with significant overlap from other activity-containing organs were also used where necessary. To estimate the activity in the lower legs (which were not imaged), an ROI on the upper thigh was used. Activities were also normalized when necessary to account for 100% of the injected activity and to ensure conservative (slight overestimates) determination of absorbed dose. Where urinary excretion data were available beyond the end of the imaging regimen, these data were used to determine whole-body retention.

Urinary Excretion Assay

Urinary excretion was collected for up to 8 h. Samples were marked for time of collection and volume of the entire void determined, and two 1-mL samples were assayed for radioactive (^{18}F) content. A known amount of ^{18}F was prepared and used as a 1-mL standard. Background counts were also determined. Activity in each urine void was then determined using Equation 1.

TABLE 1
PET Acquisition Schedule

Imaging interval (min from dose)	Scan type	Location	Acquisition time per bed position (min)*
-20 (before dosing)	Transmission	Head to mid thigh	2
0-10 [†]	Dynamic emission	Upper chest	10 s (repeated)
10-30	Emission	Head to mid thigh	2
30-50	Emission	Head to mid thigh	2
50-70	Emission	Head to mid thigh	2
70-100	Break	—	—
100-120	Transmission	Head to mid thigh	2
120-150	Emission	Head to mid thigh	3
150-180	Emission	Head to mid thigh	3
180-210	Break	—	—
210-230	Transmission	Head to mid thigh	2
230-270	Emission	Head to mid thigh	5
270-310	Emission	Head to mid thigh	5

*All head-to-mid thigh transmission and emission scans incorporated 7 bed positions.

[†]Zero time (T₀) is time of BMS747158 dose administration.

$$A_{Void} = V \left[\frac{\frac{CTS_{S1} - CTS_B}{C} + \frac{CTS_{S2} - CTS_B}{C}}{2} \right], \text{ Eq. 1}$$

where V is volume in milliliters of the total void, A_{Void} is activity in the total void, CTS_{S1} is counts recorded in sample 1, CTS_{S2} is counts recorded in sample 2, CTS_B is background counts, and C is the calibration factor (counts per unit activity based on counting standard).

Kinetic data for the brain, heart wall, kidneys, liver, red marrow (lumbar spine regions were used), salivary glands, spleen, stomach wall, thyroid, and urinary bladder for the subjects in the study were determined using the image quantification methodology. Absolute activity was converted to fractional dose by dividing by the total activity administered. Organ and tissue data were fit using nonlinear least-squares regression with sums of exponentials of the form shown in Equation 2, where f and λ are the model parameters that are determined in the fitting process, $F_{ij}(t)$ is the fraction of the total injected activity, t is the time after injection, i is the i^{th} ROI, j is the j^{th} subject, and k is the k^{th} exponential term. Between 1 and 4 exponential terms were used, as appropriate.

$$F_{ij}(t) = \sum_k f_{ijk} e^{-\lambda_{ijk} t}. \text{ Eq. 2}$$

The regression was performed using custom software that determines initial parameter values based on the temporal variation of the kinetic data and the use of pretabulated estimates for various time-activity scenarios as selected by the user. Once these data were fit, residence times were determined by integration of these empirically determined functions (sums of exponentials) from time zero to infinity, taking into account physical decay. Remainder-of-body residence times were determined by subtraction of appropriate organ residence times from whole-body residence times. Urinary bladder residence times were determined using the parameters determined by fitting the whole-body activity data with a urinary bladder model as implemented in the OLINDA/EXM software with a 3.5-h bladder-voiding interval. Red marrow residence time was determined using an ROI drawn

on a portion of the lumbar spine. The lumbar spine was assumed to contain 16.1% (17) of the total red marrow.

Organ and Tissue Dosimetry Estimates

Absorbed dose estimates for all target organs were determined using the OLINDA/EXM software with the adult male model. The resulting absorbed dose estimates were scaled using the total body mass of the individual subjects relative to that of the radiation transport phantom. Salivary gland dosimetry was determined using a conservative estimate of the S value for salivary glands based on the reference man total mass of the parotid and submaxillary salivary glands (18) and assuming a spheric shape. S values for spheres were produced by the OLINDA/EXM software and were linearly scaled on the basis of the relative total body mass of reference man to that of subject. These S values were then multiplied by the residence times to produce final salivary gland dose estimates.

Safety and Tolerability Evaluation

Subjects were closely monitored on site for 24 ± 8 h after drug administration, and safety monitoring continued for approximately 2 wk (14-17 d) after dosing. Several safety measures were included in this first-in-human study specifically to monitor for potential safety signals in the heart and brain. Multiple 12-lead ECGs were obtained at baseline and during anticipated peak BMS747158 levels and at 24 ± 8 h after dosing. Troponin-T levels were measured before and after the dose at 1, 8, and 24 h. In addition, a follow-up safety visit at approximately 1 wk (5-7 d) after dosing was conducted. Monitoring for neurophysiologic effects was conducted additionally through EEG assessments and neurologic examinations at scheduled time points before and after the dose.

An independent data-monitoring committee was established to monitor the safety of subjects participating in this clinical study. For each of the first 6 subjects enrolled, at least 1 data-monitoring committee member reviewed and assessed safety information through day 2 before the study drug was administered to the next subject. The remaining 7 subjects were enrolled with a minimum 48-h window between successive drug administrations.

The safety and tolerability endpoints were number and percentage of AEs and change from baseline in vital signs, laboratory

values, ECG, EEG, neurologic examination, and physical examination that were of clinical significance as reported by the principal investigator.

Statistical Analyses

All statistical analyses and all summary tables and listings were prepared using SAS (release 9.1.3; SAS Institute, Inc.). Standard descriptive summaries included the *N*, mean, median, SD, or coefficient of variation (%CV); minimum and maximum for continuous variables; and the number and percentage for categorical variables.

RESULTS

Patient Demography

Of the 26 subjects who were screened, 13 subjects (12 men and 1 woman) were administered BMS747158 and completed all safety evaluations. The mean age was 23.4 y (range, 19–34 y), and the mean body mass index was 23.4 (range, 20–26). One patient was not included in the analyses of dosimetry, biodistribution, and radiokinetics because of the inability to confirm the dose calibrator assay data for the standards preparation.

Radiation Dosimetry

The absorbed dose summary statistics are presented in Table 2 (mSv/MBq). The organ receiving the largest mean absorbed dose was the kidneys at 0.066 mSv/MBq (0.24 rem/mCi), followed by the heart wall at 0.048 mSv/MBq (0.18 rem/mCi). The mean ED was 0.019 mSv/MBq (0.072 rem/mCi).

Whole-Organ Biodistribution

The biodistribution of BMS747158, calculated as the whole-organ percentage injected radioactivity as a function of time, was determined for the brain, heart wall, kidneys, liver, lungs, red marrow (lumbar region), salivary glands, spleen, stomach wall, thyroid, and urinary bladder (Table 3; Fig. 3). The heart exhibited high and sustained retention of the tracer from the earliest images through approximately 5 h after injection. The liver uptake appeared to peak 10–30 min after injection and cleared by approximately 2 h. The organ that showed the largest mean peak uptake was the liver, with approximately 19.1% of the injected activity. The next largest mean peak uptake occurred in the kidneys, with approximately 9.4% of the injected activity, followed by the brain with approximately 8.3% of the injected activity. Data from subjects in the study were used to determine the urinary excretion rate for each subject and the residence time for radioactivity in the bladder using a standard model, with a theoretic fixed voiding interval of 3.5 h after dosing. The largest mean residence times were for remainder tissues (1.8 h), liver (0.28 h), and brain (0.14 h). Summary residence time statistics are presented in Table 4.

Safety and Tolerability

Three subjects (23% of total) experienced 1 non-drug-related AE each: nausea, fatigue, and a needle-associated contusion. All of these AEs were mild and required no treatment. There were no deaths, serious AEs, or other sig-

nificant AEs reported during study participation. Nausea onset was at 29 h after dosing, and fatigue onset was 49.6 h after dosing. Bruising in the right arm at the site where blood was drawn (not drug administration) occurred 23 h after dosing. All resolved within 36 h without clinical sequelae. None of the changes from baseline in hematology, coagulation, and clinical chemistry parameters were considered clinically significant. Troponin-T levels did not exhibit any clinically significant changes from baseline.

Mean ECG parameters showed no clinically significant changes from baseline through 24 ± 8 h after dosing. Three subjects (003, 004, and 016) had ECG findings of sinus bradycardia through day 2. One subject (004) had a first-degree atrioventricular block from before dosing through day 2 after dosing. One subject (005) had a nonspecific ST segment T-wave change at 2 h after dosing. None of the ECG parameter changes from baseline were considered clinically significant. No clinical abnormalities were reported on physical examination. No neurologic abnormalities or EEG changes were reported by the neurologist.

Early Elimination of ^{18}F in Urine

Urine collected before dosing (baseline) and all voids up to 8 h after dosing were collected and assayed for ^{18}F . However, as in blood collection, the urine collection terminated near the 7-h minimum specified in the protocol. Mean urinary excretion over the approximate 7-h void interval was 4.83 percentage injected dose with a %CV of 64.7 and a range of 0.64–12.41 percentage injected dose. This finding is in agreement with cumulative urine excretion of 5% as measured with PET.

DISCUSSION

This was a phase I, nonrandomized, open-label, single-dose, first-in-human study of BMS747158, with the objectives of assessing the radiation dosimetry, biodistribution, safety, tolerability, and early elimination of ^{18}F in urine, after a single-dose administration of BMS747158 at rest in healthy subjects.

Radiation Dosimetry and Biodistribution

The critical organ for BMS747158 was the kidneys, with a mean estimated dose of 0.066 mSv/MBq (0.24 rem/mCi). The maximum injected dose of the compound that may be administered without exceeding 50 mSv to the critical organ is therefore 760 MBq (20.5 mCi). This is somewhat higher than the 185 MBq (5 mCi) to 370 MBq (10 mCi) recommended in the widely used guidance by the Center for Drug Evaluation and Research, which recommends the package insert wording to facilities applying to manufacture ^{18}F -FDG (19). This difference is a result of the rapid urinary excretion of a large fraction of ^{18}F -FDG shortly after administration, resulting in a substantially higher exposure to the urinary bladder for that compound, compared with that of BMS747158. The ED due to BMS747158 (0.019 mSv/MBq) is the same as the ED due to ^{18}F -FDG (20). Because the mean estimated ED for BMS747158 is

TABLE 2
Absorbed Dose Estimates (mSv/MBq) for Void Interval of 3.5 Hours

Organ	Mean (n = 12)	%CV	Minimum	Maximum
Adrenals	1.6E-02	7	1.3E-02	1.7E-02
Brain	2.5E-02	25	1.5E-02	3.6E-02
Breasts	8.8E-03	8	7.5E-03	9.6E-03
Gallbladder wall	1.7E-02	8	1.5E-02	1.9E-02
Lower large intestine wall	1.2E-02	8	1.0E-02	1.3E-02
Small intestine	1.3E-02	8	1.1E-02	1.4E-02
Stomach wall	4.0E-02	26	2.4E-02	6.2E-02
Upper large intestine wall	1.3E-02	7	1.1E-02	1.4E-02
Heart wall	4.8E-02	17	3.4E-02	6.4E-02
Kidneys	6.6E-02	22	4.4E-02	9.5E-02
Liver	3.9E-02	19	2.7E-02	5.2E-02
Lungs	1.1E-02	7	9.7E-03	1.2E-02
Muscle	1.0E-02	8	8.7E-03	1.3E-02
Ovaries	1.2E-02	8	1.1E-02	1.3E-02
Pancreas	1.6E-02	8	1.3E-02	1.8E-02
Red marrow	1.6E-02	11	1.3E-02	1.9E-02
Osteogenic cells	1.9E-02	8	1.6E-02	2.1E-02
Salivary	3.5E-02	38	2.3E-02	6.8E-02
Skin	7.9E-03	8	6.8E-03	8.7E-03
Spleen	1.6E-02	21	1.1E-02	2.1E-02
Testes	9.2E-03	9	8.1E-03	1.0E-02
Thymus	1.1E-02	8	9.6E-03	1.2E-02
Thyroid	3.2E-02	30	1.9E-02	4.9E-02
Urinary bladder wall	2.3E-02	18	1.7E-02	3.0E-02
Uterus	1.2E-02	8	1.1E-02	1.4E-02
Total body	1.2E-02	7	1.0E-02	1.3E-02
Effective dose equivalent	2.2E-02	11	1.7E-02	2.5E-02
ED	1.9E-02	12	1.5E-02	2.4E-02

E followed by – is exponent multiple of 3 convention for decimal presentation.

0.019 mSv/MBq (0.072 rem/mCi), the maximum injected dose that may be administered without exceeding 10 mSv ED is therefore 520 MBq (14 mCi). Thus, the radiation dose from BMS747158 is comparable to or less than that from ¹⁸F-FDG.

The radiation dose estimates from this study are consistent with those derived from nonhuman primates (12), and the high and sustained retention of BMS747158 in the heart is consistent with data in both nonhuman primates and in other species (9). Although the critical organ in the pri-

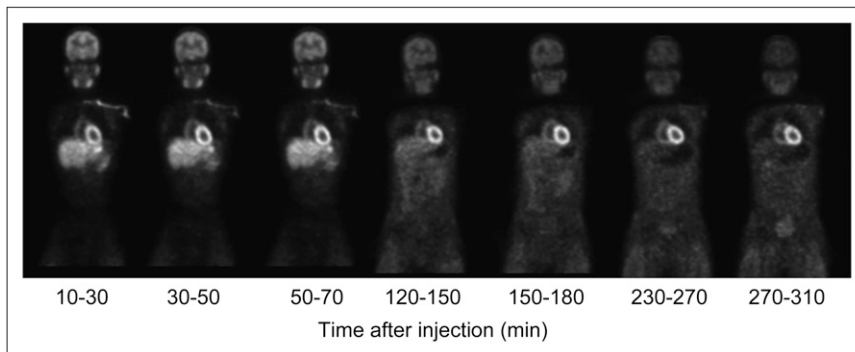
TABLE 3
Mean Percentage Decay-Corrected Administered ¹⁸F Dose Versus Time After Dosing (n = 12)

Organ	Time (h)						
	0.17*	0.50	0.83	2.0	2.5	3.83	4.5
Whole body	100.0	99.8	99.7	98.2	98.1	96.8	96.9
Brain	8.3	7.9	7.3	4.7	4.1	3.2	2.9
Gastrointestinal tract, stomach wall	2.5	2.4	2.2	0.7	0.7	0.6	0.6
Heart wall	3.1	3.2	3.4	2.4	2.5	2.1	2.1
Kidneys	9.4	6.5	4.9	1.6	1.6	1.2	1.1
Liver	19.1	18.0	16.4	7.5	7.0	4.5	4.7
Marrow (lumbar)	0.3	0.3	0.3	NA	NA	NA	NA
Salivary	0.6	0.7	0.6	0.5	0.5	0.4	0.4
Spleen	0.9	0.6	0.4	0.3	0.3	0.3	NA
Thyroid	0.1	0.1	0.1	0.1	0.1	0.1	0.1
Urinary bladder	0.3	0.2	0.3	0.9	1.1	1.4	1.7

*Nominal times in hours after dose (beginning of time window).

NA = not available.

FIGURE 3. Whole-body coronal images at level of myocardium from representative subject at different time points after administration of BMS747158. Images have been corrected for ^{18}F decay.



mate-derived estimates was seen to be the heart wall, the estimated human radiation dose for the heart wall in that study was 0.067 mSv/MBq—a value similar to the critical organ value of 0.066 mSv/MBq seen for the kidneys in this study. The doses to both organs were among the highest both in the nonhuman primate-derived results and in the current study and are within 2 SDs of one another.

Implications for Clinical MPI

Table 5 compares the radiation dose from an anticipated 111-MBq rest dose of BMS747158 with the mid points of the range of recommended rest doses for other radiopharmaceuticals used for myocardial perfusion studies (21–23). The radiation dose expected from a resting BMS747158 study is less than that of the others in terms of both critical organ and ED, except for ^{82}Rb 3-dimensional bismuth germanate imaging.

To clarify the potential of BMS747158 for rest–stress MPI in the clinical setting, some of the relevant ongoing research findings are summarized here. Dosimetry and biodistribution of BMS747158 were evaluated in 12 healthy subjects who received the tracer at rest and on a second day at peak treadmill exercise ($n = 6$) or pharmacologic stress ($n = 6$) (24). The organ receiving the highest radiation dose with adenosine and exercise stress was the heart. The ED

was 0.019 mSv/MBq with adenosine and 0.015 mSv/MBq with exercise. A total rest–stress dose of 14 mCi was determined to yield good images with clinically acceptable radiation. Myocardial uptake after stress injection remained high throughout imaging and was lower with exercise than adenosine stress because of higher skeletal muscle uptake (24). In the same subjects, it was found that a high signal-to-noise ratio can be achieved with a low dose of BMS747158 (74 MBq [2 mCi]) and short acquisition times (270 s at rest and 150 s with stress) with either dedicated PET or PET/CT in 2-dimensional mode (25). Myocardial perfusion images were not influenced by noncardiac uptake (25). More recently, it was shown that the dosage acquisition time products for 95% of patients to detect a 5% defect were 4.98 for rest, 2.94 for exercise, and 2.32 for adenosine stress images (26).

The possibility of same-day rest–stress imaging was evaluated by computer modeling (27) and phantom studies (28) and was validated in clinical studies (29). For an adenosine stress protocol, a minimum stress-to-rest dose ratio of 2.2 was required, with a 0.5-h waiting time between the 2 injections. For the same-day rest–exercise protocol, a minimum exercise-to-rest dose ratio of 3.0 was needed, with a 1-h waiting time between the 2 injections. Phase II multicenter clinical studies have been conducted using

TABLE 4
Residence Times Summary Statistics for Void Interval of 3.5 Hours

Organ	Mean (h, $n = 12$)	%CV	Minimum (h)	Maximum (h)
Brain	1.38E-01	2.69E-01	8.68E-02	2.08E-01
Gastrointestinal tract, stomach wall	3.30E-02	4.46E-01	1.53E-02	6.11E-02
Heart wall	7.28E-02	1.83E-01	4.82E-02	1.01E-01
Kidneys	9.52E-02	2.35E-01	6.10E-02	1.43E-01
Liver	2.77E-01	2.22E-01	1.83E-01	3.94E-01
Red marrow	8.86E-02	2.10E-01	6.72E-02	1.17E-01
Salivary	1.48E-02	3.24E-01	9.68E-03	2.63E-02
Spleen	1.01E-02	1.87E-01	7.26E-03	1.25E-02
Thyroid	3.31E-03	3.13E-01	1.72E-03	5.06E-03
Urinary bladder	2.65E-02	3.35E-01	1.40E-02	4.50E-02
Remainder of body	1.84E+00	7.86E-02	1.65E+00	2.08E+00

E followed by – is exponent multiple of 3 convention for decimal presentation.

TABLE 5

Radiation Dose Due to Resting Dose of Radiopharmaceuticals Used for MPI, Compared with That of BMS747158

Parameter	²⁰¹ Tl*	^{99m} Tc-sestamibi*	⁸² Rb*		BMS747158
			2-Dimensional bismuth germanate	3-Dimensional bismuth germanate	
Rest dose (MBq)	111	370	1,850	555	111
Critical organ	Ovaries	Gallbladder	Kidneys	Kidneys	Kidneys
Critical organ dose per rest study (mSv)	81	14	10.8	3.2	7.3
ED per rest study (mSv)	24	3.3	2.3	0.70	2.1

*Middle of American Society of Nuclear Cardiology guideline range was used for rest dose. Administered dose ranges for ²⁰¹Tl- and ^{99m}Tc-sestamibi are from Hansen et al. (21). Administered dose ranges for ⁸²Rb are from Machac et al. (22). Radiation dose for ²⁰¹Tl- and ^{99m}Tc-sestamibi is from ICRP 80 (20). Radiation dose from ⁸²Rb is from Senthamizhchelvan et al. (23).

these protocols. Preliminary single-center results comparing BMS747158 PET and ^{99m}Tc-labeled SPECT studies have been encouraging, suggesting that BMS747158 PET MPI demonstrates more severe and extensive stress-induced perfusion abnormalities in myocardial regions that are supplied by diseased coronary arteries (30).

Safety and Tolerability

BMS747158 was well-tolerated, and no clinically significant safety concerns were raised. Changes from baseline in vital signs, laboratory values (hematology, coagulation, clinical chemistry, and urinalysis), ECGs, and EEGs were not clinically significant. Potential cardiotoxicity (signaled through coagulation studies and changes in troponin-T levels) were not exhibited. Physical and neurologic examinations did not reveal any predose or postdose abnormalities. The data-monitoring committee did not raise safety concerns after periodic reviews of the safety data.

CONCLUSION

The results obtained in this phase I study demonstrated that BMS747158 appeared to be safe and was well tolerated and exhibited a substantial and sustained retention in the myocardium. The critical organ after a resting injection of BMS747158 was the kidneys, with 0.066 mSv/MBq. On the basis of the observed mean ED, the maximum injected dose that may be administered without exceeding 1 rem ED is 14 mCi (520 MBq). The ED from BMS747158 is the same as that of ¹⁸F-FDG, whereas the critical organ (kidney) dose of BMS747158 is significantly less than the critical organ (urinary bladder) dose of ¹⁸F-FDG. Studies are currently under way to assess further the safety of this promising tracer, its myocardial imaging characteristics, and its application in evaluation of coronary artery disease.

DISCLOSURE STATEMENT

The costs of publication of this article were defrayed in part by the payment of page charges. Therefore, and solely

to indicate this fact, this article is hereby marked "advertisement" in accordance with 18 USC section 1734.

ACKNOWLEDGMENTS

We acknowledge the assistance of Jean-Richard Eugene, CNMT, in PET image acquisition and processing, Deborah Dorsey, and Parham Naghdechi in recruitment and monitoring of the research subjects. We are grateful to Susan Ramsey for analyzing the data and for helpful comments on drafts of the manuscript. Financial support for this study was provided by Lantheus Medical Imaging, Billerica, MA. No other potential conflict of interest relevant to this article was reported.

REFERENCES

- Schwaiger M. Myocardial perfusion imaging with PET. *J Nucl Med.* 1994; 35:693–698.
- Bateman TM, Heller GV, McGhie AI, et al. Diagnostic accuracy of rest/stress ECG-gated Rb-82 myocardial perfusion PET: comparison with ECG-gated Tc-99m sestamibi SPECT. *J Nucl Cardiol.* 2006;13:24–33.
- Di Carli MF, Dorbala S, Meserve J, El Fakhri G, Sitek A, Moore SC. Clinical myocardial perfusion PET/CT. *J Nucl Med.* 2007;48:783–793.
- Huang SC, Williams BA, Krivokapich J, Araujo L, Phelps ME, Schelbert HR. Rabbit myocardial ⁸²Rb kinetics and a compartmental model for blood flow estimation. *Am J Physiol.* 1989;256:H1156–H1164.
- Schelbert HR, Phelps ME, Huang SC, et al. N-13 ammonia as an indicator of myocardial blood flow. *Circulation.* 1981;63:1259–1272.
- Bergmann SR, Herrero P, Markham J, et al. Noninvasive quantitation of myocardial perfusion in human subjects with O-15 labeled water and positron emission tomography. *J Am Coll Cardiol.* 1989;14:639–652.
- Glover DK, Gropler RJ. Journey to find the ideal PET flow tracer for clinical use: are we there yet? *J Nucl Cardiol.* 2007;14:765–768.
- Yalamanchili P, Wexler E, Hayes M, et al. Mechanism of uptake and retention of ¹⁸F BMS747158-02 in cardiomyocytes: a novel PET myocardial imaging agent. *J Nucl Cardiol.* 2007;14:782–788.
- Yu M, Guaraldi MT, Mistry M, et al. BMS747158-02: a novel PET myocardial perfusion imaging agent. *J Nucl Cardiol.* 2007;14:789–798.
- Huisman M, Higuchi T, Reder S, et al. Initial characterization of an ¹⁸F-labeled myocardial perfusion tracer. *J Nucl Med.* 2008;49:630–636.
- Nekolla SG, Reder S, Higuchi T, et al. Evaluation of the novel myocardial perfusion PET tracer ¹⁸F-BMS747158-02: comparison to ¹³N ammonia and validation with microspheres in a pig model. *Circulation.* 2009;119:2333–2342.
- Lazewatsky J, Azure M, Guaraldi M, et al. Dosimetry of BMS747158, a novel ¹⁸F labeled tracer for myocardial perfusion imaging, in nonhuman primates at rest [abstract]. *J Nucl Med.* 2009;49(suppl 1):15P.

13. International Commission on Radiological Protection (ICRP). Recommendations of the International Commission on Radiological Protection. Publication 26. *Ann ICRP*. 1977;1:21.
14. International Commission on Radiological Protection (ICRP). Recommendations of the International Commission on Radiological Protection. Publication 60. *Ann ICRP*. 1990;21:7–9.
15. Stabin MG, Sparks RB, Crowe E. OLINDA/EXM: the second-generation personal computer software for internal dose assessment in nuclear medicine. *J Nucl Med*. 2005;46:1023–1027.
16. Siegel JA, Thomas SR, Stubbs JB, et al. MIRD pamphlet no. 16: techniques for quantitative radiopharmaceutical biodistribution data acquisition and analysis for use in human radiation dose estimates. *J Nucl Med*. 1999;40:37S–61S.
17. International Commission on Radiological Protection (ICRP). Basic anatomical and physiological data for use in radiological protection: the skeleton. *Ann ICRP*. 1995;21:66.
18. International Commission on Radiological Protection (ICRP). *Report of the Task Group on Reference Man*. Publication 23. Oxford, U.K.: Pergamon Press; 1975.
19. PET Drug Applications—Content and Format for NDAs and ANDAs. Fludeoxyglucose F 18 Injection, Ammonia N 13 Injection, Sodium Fluoride F 18 Injection, Attachment II, Sample Formats; Labeling for Ammonia N 13 Injection, Fludeoxyglucose F 18 Injection and Sodium Fluoride F 18 Injection, Attachment II (CDER 2000). Washington, DC: United States Food and Drug Administration; 2000.
20. International Commission on Radiological Protection (ICRP). Radiation dose to patients from radiopharmaceuticals, addendum 2 to ICRP publication 53. Publication 80. *Ann ICRP*. 1999;28.
21. Hansen CL, Goldstein RA, Akinboboye OO, et al. Myocardial perfusion and function: single photon emission computed tomography. *J Nucl Cardiol*. 2007;14:e39–e60.
22. Machac J, Bacharach SL, Bateman TM, et al. Positron emission tomography myocardial perfusion and glucose metabolism imaging. *J Nucl Cardiol*. 2006;13:e121–e151.
23. Senthamizhchelvan S, Bravo PE, Esaías C, Sgouros G, Bengel FM. Human biodistribution and radiation dosimetry of ⁸²Rb. *J Nucl Med*. 2010;51:1592–1599.
24. Maddahi J, Bengel F, Huang H, et al. Phase 1 rest-stress study of F-18 labeled BMS747158 myocardial perfusion PET tracer: human safety, dosimetry, biodistribution, and myocardial imaging characteristics [abstract]. *J Nucl Med*. 2009;50:48P.
25. Case JA, Maddahi J, Bengel FM, Bateman T, Dahlbom M, Lazewatsky J. Imaging properties of F-18 labeled myocardial perfusion PET agent, BMS747158: dosage, acquisition time and scanner type [abstract]. *J Nucl Med*. 2009;50:109P.
26. Case JA, Lazewatsky JL, Hsu BL, Maddahi J, Berman DS, Bateman TM. Iterative technique for optimizing injected tracer dosage and acquisition time for F-18 labeled myocardial perfusion tracer flurpiridaz F-18 [abstract]. *J Nucl Cardiol*. 2010;17:726.
27. Maddahi J, Huang S, Schiepers C, et al. Same day rest-stress protocols for PET imaging with the new F-18 labeled BMS747158 myocardial perfusion trace [abstract]. *J Nucl Med*. 2009;50:219P.
28. Hsu B, Lazewatsky JL, Bateman T, et al. Cardiac phantom simulation of dose injection parameters for one-day rest/stress myocardial perfusion (MPI) PET imaging with BMS747158 tracer [abstract]. *J Nucl Med*. 2010;51:89P.
29. Lazewatsky J, Maddahi J, Berman D, et al. Development of a method for the determination of dose ratio and minimum inter-injection interval for a one-day rest-stress protocol with BMS747158 PET myocardial perfusion agent [abstract]. *J Nucl Med*. 2010;51:166P.
30. Maddahi J, Lee M, Czernin J, et al. F-18 labeled BMS747158 PET myocardial perfusion imaging identifies more severe and extensive stress induced myocardial ischemia than Tc-99m Sestamibi SPECT [abstract]. *J Nucl Med*. 2010; 51:365P.

Errata

In the article “Novel ⁶⁴Cu- and ⁶⁸Ga-Labeled RGD Conjugates Show Improved PET Imaging of $\alpha_v\beta_3$ Integrin Expression and Facile Radiosynthesis,” by Dumont et al. (*J Nucl Med*. 2011;52:1276–1284), support by Deutsche Forschungsgemeinschaft SFB 850 Project B7 was inadvertently omitted from the Acknowledgments. The authors regret the error.

In the article “MIRD Pamphlet No. 20: The Effect of Model Assumptions on Kidney Dosimetry and Response—Implications for Radionuclide Therapy,” by Wessels et al. (*J Nucl Med*. 2008;49:1884–1889), term “C” in Equation 7B was missing. The corrected equation and preceding sentence should read as follows:

Similarly, the exact expression for times less than infinity (for $D_T = [R_0/\lambda_e]C$) is given by

$$\text{BED} = \frac{R_0}{\lambda_e} C \left[1 + \frac{2R_0\lambda_e}{[(\mu - \lambda_e)(\alpha/\beta)]} \frac{A - B}{C} \right], \quad (\text{Eq. 7B})$$

$$\text{where } A = \frac{1 - e^{-2\lambda_e T}}{2\lambda_e}; B = \frac{1 - e^{-(\mu + \lambda_e)T}}{\mu + \lambda_e}; \text{ and } C = 1 - e^{-\lambda_e T}$$

The authors regret the error; they and the MIRD Committee wish to thank Drs. Katarina Sjögreen Gleisner of the University of Lund, Sweden, and Peter Roberson of the University of Michigan for bringing this correction to their attention.